Phase Models Beyond Weak Coupling

Dan Wilson and Bard Ermentrout

Phys. Rev. Lett. **123**, 164101 — Published 15 October 2019

DOI: 10.1103/PhysRevLett.123.164101

Phase Models Beyond Weak Coupling

Dan Wilson*
Department of Electrical Engineering and Computer Science, University of Tennessee, Knoxville,TN 37996

Bard Ermentrout†
Department of Mathematics, University of Pittsburgh,Pittsburgh PA 15260

(Dated: September 11, 2019)

We use the theory of isostable reduction to incorporate higher order effects that are lost in the first order phase reduction of coupled oscillators. We apply this theory to weakly coupled complex Ginzburg-Landau equations, a pair of conductance-based neural models, and finally to a short derivation of the Kuramoto-Sivashinsky equations. Numerical and analytical examples illustrate bifurcations occurring in coupled oscillator networks that can cause standard phase reduction methods to fail.

Self-sustaining oscillatory behaviors can widely be observed in the physical, chemical and biological sciences [1], [2]. Phase reduction is a tremendously powerful tool to represent the timing of a high-dimensional limit cycle oscillation, [1], [3], [4], and has been extensively used to study the dynamics of coupled oscillators in the weakly coupled limit. Studies using phase reduction as a starting point have been used successfully to elegantly characterize complicated patterns that emerge in groups of weakly interacting oscillators [5], [6], [7], [8].

While phase reduction is useful in many applications, its applicability degrades as coupling strength increases, often leading to incorrect predictions about dynamical behavior. Due to this limitation, recent years have seen a flurry of interest in the development and use of nonlinear model reduction strategies to characterize the dynamical behavior of coupled limit cycle oscillators in situations where the weak coupling approximation is not sufficient [9], [10], [11], [12], [13], [14], [15], [16]. In general, this is a difficult task for an n-dimensional model as greater accuracy coupling functions must usually be found by considering the dynamical behavior of $n-1$ coordinates transverse to a limit cycle.

In this letter, we approach this problem from the perspective of phase-isostable reduced coordinates [17], [13], in which Floquet theory [18] provides a foundation from which to define a set of globally exponentially decaying coordinates in an analytically tractable nonlinear reduction framework. Subsequent analysis is used to predict and illustrate bifurcations that emerge as coupling strength increases in high-dimensional systems of coupled oscillators. As shown in examples to follow, this phase-isostable reduction framework can be implemented analytically for some models. Additionally, the general framework presented here can be used as a starting point for future research on the behavior of limit cycle oscillators beyond the weak coupling limit.

We consider the dynamics of N identical coupled oscillators:

$$X_i' = F(X_i) + \epsilon \sum_{j=1}^{N} a_{ij} G(X_i, X_j), \quad X_i \in R^n, i = 1, \dots N. \tag{1}$$

where $' \equiv d/dt$, $0 < \epsilon \ll 1$, G denotes coupling interactions that are of the same form between oscillators and only differ with respect to weights, a_{ij} and F gives the uncoupled dynamics so that $X' = F(X)$ has a stable P-periodic limit cycle, $Y(t)$. For simplicity of exposition, we assume that all but one of the $n-1$ nonzero Floquet multipliers is sufficiently close to 0 so that only a single isostable coordinate is required per oscillator (cf., [17]). Let $\kappa < 0$ be the corresponding Floquet exponent and $\rho(t)$ the corresponding eigenfunction and introduce the phase, θ_i and (isostable) amplitude, ψ_i coordinates, $X_i(t) = Y(\theta_i(t)) + \psi_i(t)\rho(\theta_i(t))$. Here, $\theta_i \in \mathbb{S}^1$ and $\psi_i \in \mathbb{R}$ gives the distance from the periodic orbit parameterized by ρ. Letting $U_i(t) \equiv \sum_{j=1}^{N} a_{ij} G(X_i, X_j)$ denote the sum of coupling inputs we can use the theory of isostable reduction [17], [13] to get:

$$\begin{aligned} \theta_i' &= 1 + \epsilon[Z(\theta_i) + \psi_i B(\theta_i)]U_i(t), \\ \psi_i' &= \kappa\psi_i + \epsilon[I(\theta_i) + \psi_i C(\theta_i)]U_i(t), \end{aligned} \tag{2}$$

The four functions Z, I, B, C are all computable from the ordinary differential equation $X' = F(X)$ by solving an appropriate boundary value problem [13]. The function $Z(\theta)$ is the phase-sensitivity function (cf., [1] Eq. 3.2.8). A related phase-amplitude approach was considered in [15] to analyze oscillatory dynamics subject to noise. Since ψ_i are small $G(X_i, X_j) \approx G(Y(\theta_i), Y(\theta_j)) + \psi_i \rho(\theta_i) G_1(Y(\theta_i), Y(\theta_j)) + \psi_j \rho(\theta_j) G_2(Y(\theta_i), Y(\theta_j))$ where $G_{1,2}$ are the partial derivatives of G with respect to its two arguments. Keeping only the lowest order terms, we use the definition of U_i to see that

$$\begin{aligned} \theta_i' &= 1 + \epsilon \sum_j a_{ij}[Z(\theta_i) \cdot G(Y(\theta_i), Y(\theta_j)) \\ &\quad + \psi_i h_2(\theta_i, \theta_j) + \psi_j h_3(\theta_i, \theta_j)], \\ \psi_i' &= \kappa\psi_i + \epsilon \sum_j a_{ij} I(\theta_i) \cdot G(Y(\theta_i), Y(\theta_j)), \end{aligned} \tag{3}$$

* dwilso81@utk.edu
† bard@pitt.edu

where

$$h_2(\theta_i,\theta_j) = Z(\theta_i)\cdot G_1(Y(\theta_i),Y(\theta_j))\rho(\theta_i) + B(\theta_i)\cdot G(Y(\theta_i),Y(\theta_j)),$$
$$h_3(\theta_i,\theta_j) = Z(\theta_i)\cdot G_2(Y(\theta_i),Y(\theta_j))\rho(\theta_j).$$

If we neglect the amplitude, ψ_i, then we obtain the usual first order phase reduction.

Substituting $\theta_i = t+\phi_i$ and $\psi_i = \epsilon r_i$ into Eq. (3) we solve the resulting linear equation for r_i:

$$r_j = \sum_k a_{jk}\int_0^\infty e^{\kappa s} I(\theta_j - s)\cdot G(Y(\theta_j - s), Y(\theta_k - s))ds \equiv \sum_k a_{jk} f_4(\theta_j,\theta_k).$$

Plugging this into the equation for ϕ_i we get

$$\phi_i' = \epsilon\sum_j a_{ij} Z(t+\phi_i)\cdot G(Y(t+\phi_i),Y(t+\phi_j)) + \epsilon^2\sum_j a_{ij}\big[r_i(t)h_2(t+\phi_i,t+\phi_j) + r_j(t)h_3(t+\phi_i,t+\phi_j)\big].$$

Finally, we average the right hand sides over a period P:

$$\phi_i' = \epsilon\sum_j a_{ij}H_1(\phi_j-\phi_i) + \epsilon^2\sum_{jk}\left[a_{ij}a_{ik}H_{24}(\phi_j-\phi_i,\phi_k-\phi_i) + a_{ij}a_{jk}H_{34}(\phi_j-\phi_i,\phi_k-\phi_i)\right], \quad (4)$$
$$H_1(\eta) = \langle Z(t)\cdot G(Y(t),Y(t+\eta))\rangle,$$
$$H_{24}(\eta,\xi) = \langle f_4(t,t+\xi)h_2(t,t+\eta)\rangle,$$
$$H_{34}(\eta,\xi) = \langle f_4(t+\eta,t+\xi)h_3(t,t+\eta)\rangle,$$

where $\langle f(t)\rangle = (1/P)\int_0^P f(t)dt$.

N=2. When $N=2$, and coupling is symmetric, then $a_{11}=a_{22}=0$ and $a_{12}=a_{21}=1$ and we get

$$\phi_i' = \epsilon H_1(\phi_j-\phi_i)+\epsilon^2[H_{24}(\phi_j-\phi_i,\phi_j-\phi_i)+H_{34}(\phi_j-\phi_i,0)],$$

where $i=1,2$ and $j=2,1$ Finally, this system of 2 equations reduces to a single equation for the phase-difference, $\phi=\phi_2-\phi_1$:

$$\phi' = \epsilon[g_1(\phi)+\epsilon(g_2(\phi)+g_3(\phi))], \quad (5)$$

where $g_1(\phi) = H_1(-\phi)-H_1(\phi)$, $g_2(\phi) = H_{24}(-\phi,-\phi) - H_{24}(\phi,\phi)$ and $g_3(\phi) = H_{34}(-\phi,0) - H_{34}(\phi,0)$. Stable equilibria of Eq. (5) correspond to stable locking of the coupled oscillator system. For example, it is clear that perfect synchrony, $\phi=0$ is always a solution since the functions $g_k(\phi)$ are odd and periodic. Synchrony will be stable if $g_1'(0)+\epsilon[g_2'(0)+g_3'(0)]<0$. If $g_1'(0)$ is near 0, then, the higher order terms have a significant role in determining stability and can also introduce additional fixed points. We will see both of these phenomena in the examples below.

We also remark that if $G(X_1,X_2) = D(X_2-X_1)$, i.e., diffusive coupling, then:

$$H_1(\phi) = \langle Z(t)\cdot D(Y(t+\phi)-Y(t))\rangle, \quad (6)$$
$$H_{24}(\phi,\phi) = \langle f_4(t,t+\phi)[-Z(t)\cdot D\rho(t) + B(t)\cdot D(Y(t+\phi)-Y(t))]\rangle,$$
$$H_{34}(\phi,0) = \langle f_4(t+\phi,t)Z(t)\cdot D\rho(t+\phi)\rangle.$$

Complex Ginzburg-Landau Model: Consider a pair of coupled CGL oscillators (in real coordinates):

$$x_j' = x_j(1-x_j^2-y_j^2) - q(x_j^2+y_j^2)y_j + \epsilon[x_k - x_j - d(y_k-y_j)], \quad (7)$$
$$y_j' = y_j(1-x_j^2-y_j^2) + q(x_j^2+y_j^2)x_j + \epsilon[y_k - y_j + d(x_k-x_j)],$$

for $j=1,2$ and $k=3-j$. With $\epsilon=0$, this system admits a periodic solution, $Y=(\cos qt,\sin qt) := (C,S)$ and the relevant functions are $Z=(S-S/q, S+C/q)$, $\rho=(qS+C, S-qC)$, $I=(C,S)$ and $B=\frac{1+q^2}{q}(S,-C)$. Additionally, $P=2\pi/q$ and $\kappa=-2$. Note here that because the natural frequency is scaled to be 1 in Eq. (2) the phase takes values in the range of 0 to P. We can then evaluate Eq. (5) and from these obtain the locking equation:

$$\phi' = -\epsilon\frac{2}{q}\sin q\phi\left(1-dq+\epsilon d^2(1+q^2)\cos q\phi\right). \quad (8)$$

The standard phase reduction ignores the $O(\epsilon^2)$ terms and shows exactly two fixed points $\phi=0$ (synchrony) and $\phi=\pi/q$ (anti-phase). If $\epsilon>0$ then synchrony (anti-phase) is stable if and only if $1-dq>0$ (resp. $1-dq<0$) and when $\epsilon<0$, these are reversed. The coupled CGL model allows for an exact expression for all the locking regions and their stability [19]. The true critical curves for the stability of synchrony (s) and anti-phase (a) are:

$$\epsilon_s = \frac{dq-1}{d^2+1},$$
$$\epsilon_a = \frac{1-dq}{d^2-2dq+3}, \quad (9)$$

along with $\epsilon=0$. These curves are shown in Fig. 1 for $q=1$. In particular, there are additional fixed points and also bistability between synchrony and anti-phase for finite non-zero coupling as shown by the shaded regions. Using the higher order locking Eq. (8), we can compute the stability of synchrony and anti-phase to get the approximate curves:

$$\epsilon_{s,approx} = \frac{dq-1}{d^2(1+q^2)},$$
$$\epsilon_{a,approx} = \frac{1-dq}{d^2(1+q^2)}. \quad (10)$$

These are shown by the thick solid and dashed lines in the figure. The agreement is good near the bifurcation

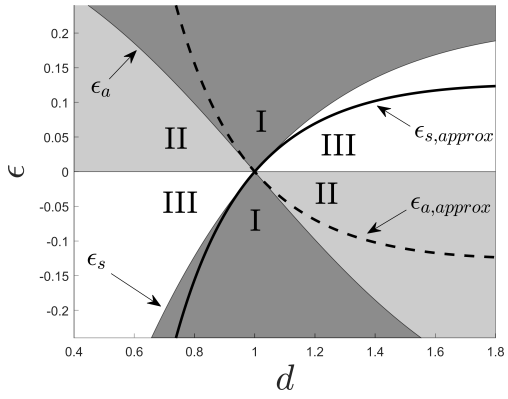

FIG. 1. Above, the intersection of ϵ_a and ϵ_s as given by (9) define regions for which locking (either synchronous or antiphase) is stable for the CGL model (7) when $q = 1$ and (d, ϵ) vary. Synchrony is only stable in regions I,II; anti-phase is only stable in I,III. Thick solid and dashed lines show $\epsilon_{s,approx}$ and $\epsilon_{a,approx}$, respectively, determined from the higher order phase approximation.

point $d = 1$ (when $1 - dq = 0$) where they are tangent to the true curves. Furthermore, all regions are captured qualitatively.

Loss of Bistability in a Conductance Based Neural Model: Here we use (5) to analyze phase locking in a conductance based model of synaptically coupled neurons [20]:

$$\begin{aligned} CV_i' &= -I_L(V_i) - I_{Na}(V_i, h_i) - I_K(V_i, h_i) - I_T(V_i, r_i) \\ &\quad + I_b - \epsilon \textstyle\sum_{j\neq i} I_{syn}(V_i, w_j), \\ h_i' &= (h_\infty(V_i) - h_i)/\tau_h(V_i), \\ r_i' &= (r_\infty(V_i) - r_i)/\tau_r(V_i), \\ w_i' &= \alpha(1 - w_i)/(1 + \exp(-(V_i - V_T)/\sigma_T)) - \beta w_i. \end{aligned} \tag{11}$$

with $i = 1, 2$. Here, V_i denotes the transmembrane voltage of the i^{th} neuron, h_i and r_i are associated gating variables, and w_i is a synaptic variable. Leak, sodium, potassium, low-threshold calcium current, and baseline current are $I_L = g_L(V_i - E_L)$, $I_{Na} = g_{Na} m_\infty^3(V_i) h_i (V_i - E_{Na})$, $I_K = g_K(.75(1 - h_i))^4(V_i - E_K)$, $I_T = g_T p_\infty^2(V_i) r_i (V_i - E_T)$, and $I_b = 2.9\mu\text{A/cm}^2$, respectively. We take $g_L = 0.15$, $g_{Na} = 3$, $g_K = 5$, and $g_T = 10$ mS/cm^2, reversal potentials are $E_L = -75$, $E_{Na} = 3$, $E_K = -90$, and $E_T = 0$ mV, and $C = 1\mu\text{F/cm}^2$. Synaptic current $I_{\text{syn}}(V_i, w_j) = w_j(V_i - V_{syn})$, $V_{syn} = 0$ mV, $\alpha = 3\text{ms}^{-1}$, $V_T = -20$ mV, $\sigma_T = 0.8$ mV, and $\beta = 0.15\text{ms}^{-1}$ and ϵ sets the magnitude of the coupling. All other functions are identical to those from [20].

In the absence of coupling, each neuron settles to a limit cycle solution with period $P = 24.2$ ms. The limit cycles have one nonnegligible Floquet multiplier of 0.67 (the exponent, $\kappa = -0.01654$/msec), the remaining Floquet multipliers are close to zero so that they can be ignored from the reduction (2). Using methods described in [13] the reduced functions Z, B, I, and C from (2) are calculated numerically and subsequently used to determine the functions H_1, H_{24}, H_{34} and f_4 from (4). First and second order coupling functions calculated numerically and shown in panels B and D of Fig. 2 for different values of ϵ. For low coupling strengths (in the limit of small coupling), both first and second approximations (gray and blue curves, respectively) predict bistability of (11) whereby both the synchronous and anti-phase states are stable. Panel A confirms this in full model simulations. However, as ϵ increases, the synchronous state loses stability, as seen in panel C. This behavior is predicted from the second order accurate approximation from panel D. Note that (5) does not necessarily characterize the transient convergence to the limiting solution; application of Floquet theory to the synchronized limit cycle solution of (11) identifies a pair of complex conjugate Floquet exponents. This explains the intersecting black lines in panel A.

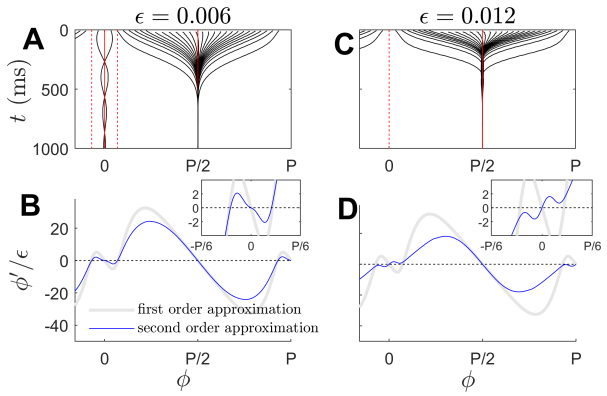

FIG. 2. Solid black lines in Panels A and C show the phase differences from full simulations of (11) for different initial conditions and coupling strengths. Here, ϕ is inferred directly from from numerical simulations of the full model (11). Panels B and D illustrate corresponding coupling functions calculated according to (5). Dashed (resp., solid) red lines denote unstable (resp. stable) fixed points predicted by the second order accurate coupling functions. The loss of stability due to changes in coupling strength can never be predicted by first order accurate methods alone because the shape of the resulting coupling function cannot change with ϵ. On the other hand, the second order accurate strategy used here reflects the observed behavior perfectly.

A Concise Derivation of the Kuramoto-Sivashinsky Equations: We can use the isostable formulation to analyze weakly coupled PDEs as well as ODEs by assuming spatial dependence in the phase and isostable coordinates. For example, the KS equation arises from a perturbative analysis of the equation:

$$u_t(x, t) = F(u) + \epsilon D u_{xx},$$

when $u_t = F(u)$ has a stable periodic orbit, $Y(t)$. (Note the analysis is the same in multiple space dimensions.)

In this case, $u(x,t) \approx Y(t+\phi(x,t))$ and ϕ solves:

$$\phi_t = \epsilon\left(\beta\phi_x^2 + \alpha\phi_{xx} + \gamma\phi_{xxxx}\right),$$

where [1]

$$\alpha = \langle Z(t)\cdot DY'(t)\rangle,$$
$$\beta = \langle Z(t)\cdot DY''(t)\rangle.$$

Here we also show that the the coefficient γ can be directly related to the terms of the phase amplitude equations (2). Recall the first order phase equation for a pair of diffusively coupled oscillators Eq (6). We can use these to see $\alpha = H_1'(0)$ and $\beta = H_1''(0)$. If α is $O(1)$, then the fourth derivative terms do not come into play; however, if α is small, then they matter. To emphasize this point, we write $D = D_0 + \epsilon D_1$ so that $\alpha = \alpha_0 + \epsilon\alpha_1$ and D_0 is chosen so that $\alpha_0 = 0$. (Note that D cannot be a scalar multiple of the identity since $\langle Z(t)\cdot Y'(t)\rangle = 1$. We also assume that D_1 is not a multiple of D_0 so that α is not 0 for $\epsilon \neq 0$.) The coefficient γ is quite complicated to compute (see Eq. 4.2.26 in [1]). We now show that it is directly related to the second order phase functions. To simplify the analysis, as above, we assume a single isostable coordinate. As in the discretely coupled systems, we write

$$u(x,t) = Y(\theta) + \psi\rho(\theta),$$

so that

$$u_{xx} = Y''(\theta)\theta_x^2 + Y'(\theta)\theta_{xx} + 2\psi_x\theta_x\rho'(\theta) + \psi_{xx}\rho(\theta) + \psi\theta_x^2\rho''(\theta) + \psi\theta_{xx}\rho'(\theta).$$

With this, we can write the isostable equations for the PDE:

$$\theta_t = 1 + \epsilon[Z(\theta) + \psi B(\theta)]\cdot(D_0 + \epsilon D_1)u_{xx},$$
$$\psi_t = \kappa\psi + \epsilon[I(\theta) + \psi C(\theta)]\cdot(D_0 + \epsilon D_1)u_{xx}.$$

Our assumption on D_0 ($\alpha_0 = 0$) enables us to make the ansatz, $\theta = t + \epsilon\phi$ and $\psi = \epsilon^2 r$, whence,

$$u_{xx} = \epsilon Y'(\theta)\phi_{xx} + \epsilon^2[Y''(\theta)\phi_x^2 + r_{xx}\rho(\theta)] + O(\epsilon^3).$$

(We remark that the scaling of ϕ, ψ has changed by order ϵ here. This is a consequence of our assuming that α is not $O(1)$, but rather $O(\epsilon)$ and is made in order for the order ϵ terms to ultimately vanish.) Proceeding as above, we find

$$r(x,\theta) = \phi_{xx}\int_0^\infty e^{\kappa s} I(\theta - s) D_0 Y'(\theta - s)\, ds \equiv \phi_{xx} f_4(\theta).$$

and plugging into the equation for ϕ, we get:

$$\phi_t = \epsilon Z(\theta)\cdot D_0 Y'(\theta)\phi_{xx} + \epsilon^2 Z(\theta)\cdot\left(D_1 Y'(\theta)\phi_{xx} + D_0[Y''(\theta)\phi_x^2 + \rho(\theta)f_4(\theta)\phi_{xxxx}]\right)$$

Averaging this over θ, we obtain the KS equations with $\alpha = \alpha_1 = \langle Z(t)\cdot D_1 Y'(t)\rangle$, $\beta = \langle Z(t)\cdot D_0 Y''(t)\rangle$ and

$$\gamma = \left\langle \int_0^\infty ds\, e^{\kappa s} I(t-s)\cdot D_0 Y'(t-s) Z(t)\cdot D_0\rho(t)\right\rangle.$$

Recalling the definitions of H_{24} and H_{34} from Eq. (6) above, we see that

$$\gamma = -\frac{\partial H_{34}(\phi,0)}{\partial\phi}|_{\phi=0} = -\frac{\partial H_{24}(\phi,\phi)}{\partial\phi}|_{\phi=0} = \frac{1}{4}(g_2'(0) + g_3'(0)).$$

Remarkably, while $B(\theta)$ plays a role in higher order diffusive coupling, it is irrelevant to γ. This calculation can be generalized to the case of multiple isostables with the same result: the coefficient γ is just one fourth of the slope of the higher order phase-interaction function evaluated at synchrony.

Conclusions To conclude, we have developed a framework that can be used to determine the coupling functions with accuracy beyond that of the standard phase reduced framework. Our analysis indicates that the coupling strength can have a profound influence on the shape of coupling functions, ultimately resulting in qualitative differences in steady state behavior that first order phase reduction methods are unable to predict. Numerical examples presented here illustrate the necessity of incorporating higher order effects when the dynamics are close to a bifurcation. Due to the generality of the approach presented here, we expect this method to shed light on the mechanisms governing synchronization in larger populations of limit cycle oscillators. Interesting future extensions will consider limiting behavior with $N > 2$ oscillators that can yield richer limiting behaviors (e.g., rotating block and chimera states). Finally, the results presented here are accurate to $\mathcal{O}(\epsilon^2)$ in the coupling strength. In order to understand bifurcations that occur at even higher coupling strengths other methods that give a fuller representation of the phase and amplitude coordinates will need to be used.

Acknowledgments This work was supported by National Science Foundation grants CMMI-1933583 and DMS-1712922.

[1] Y. Kuramoto, *Chemical Oscillations, Waves, and Turbulence* (Springer-Verlag, Berlin, 1984).

[2] A. Winfree, *The Geometry of Biological Time*, 2nd ed. (Springer Verlag, New York, 2001).

[3] E. M. Izhikevich, *Dynamical Systems in Neuroscience: The Geometry of Excitability and Bursting* (MIT Press, London, 2007).

[4] G. B. Ermentrout and D. H. Terman, *Mathematical Foundations of Neuroscience*, Vol. 35 (Springer, New York, 2010).

[5] S. H. Strogatz, D. M. Abrams, A. McRobie, B. Eckhardt, and E. Ott, Theoretical mechanics: Crowd synchrony on the millennium bridge, Nature **438**, 43 (2005).

[6] F. Dörfler, M. Chertkov, and F. Bullo, Synchronization in complex oscillator networks and smart grids, Proceedings of the National Academy of Sciences **110**, 2005 (2013).

[7] D. M. Abrams and S. H. Strogatz, Chimera states for coupled oscillators, Physical Review Letters **93**, 174102 (2004).

[8] A. V. Pimenova, D. S. Goldobin, M. Rosenblum, and A. Pikovsky, Interplay of coupling and common noise at the transition to synchrony in oscillator populations, Scientific reports **6**, 38518 (2016).

[9] W. Kurebayashi, S. Shirasaka, and H. Nakao, Phase reduction method for strongly perturbed limit cycle oscillators, Physical Review Letters **111**, 214101 (2013).

[10] Y. Park and B. Ermentrout, Weakly coupled oscillators in a slowly varying world, Journal of Computational Neuroscience **40**, 269 (2016).

[11] K. Pyragas and V. Novičenko, Phase reduction of a limit cycle oscillator perturbed by a strong amplitude-modulated high-frequency force, Physical Review E **92**, 012910 (2015).

[12] J. N. Teramae, H. Nakao, and G. B. Ermentrout, Stochastic phase reduction for a general class of noisy limit cycle oscillators, Physical Review Letters **102**, 194102 (2009).

[13] D. Wilson, Isostable reduction of oscillators with piecewise smooth dynamics and complex Floquet multipliers, Physical Review E **99**, 022210 (2019).

[14] M. Rosenblum and A. Pikovsky, Numerical phase reduction beyond the first order approximation, Chaos: An Interdisciplinary Journal of Nonlinear Science **29**, 011105 (2019).

[15] D. S. Goldobin, J. Teramae, H. Nakao, and G. B. Ermentrout, Dynamics of limit-cycle oscillators subject to general noise, Physical Review Letters **105**, 154101 (2010).

[16] D. S. Goldobin and A. V. Dolmatova, Interplay of the mechanisms of synchronization by common noise and global coupling for a general class of limit-cycle oscillators, Communications in Nonlinear Science and Numerical Simulation **75**, 94 (2019).

[17] D. Wilson and B. Ermentrout, Greater accuracy and broadened applicability of phase reduction using isostable coordinates, Journal of Mathematical Biology **76**, 37 (2018).

[18] D. Jordan and P. Smith, *Nonlinear Ordinary Differential Equations: An Introduction for Scientists and Engineers*, Vol. 10 (Oxford University Press, Oxford, 2007).

[19] D. G. Aronson, G. B. Ermentrout, and N. Kopell, Amplitude response of coupled oscillators, Physica D **41**, 403 (1990).

[20] J. Rubin and D. Terman, High frequency stimulation of the subthalamic nucleus eliminates pathological thalamic rhythmicity in a computational model, Journal of Computational Neuroscience **16**, 211 (2004).